

## **Session III**

### **ANDES**

*Chair: Arjan Plompen*



## Measurement of (n,xn $\gamma$ ) reactions of interest for new nuclear reactors

Maëlle Kerveno,<sup>1</sup> Catalin Borcea,<sup>2</sup> Philippe Dessagne,<sup>1</sup> Jean-Claude Drohé,<sup>3</sup> Erwin Jericha,<sup>4</sup>  
Habib Karam,<sup>1</sup> Arjan J. Koning,<sup>5</sup> Alexandru Negret,<sup>2</sup> Andreas Pavlik,<sup>6</sup> Arjan J.M. Plompen,<sup>3</sup>  
Chariklia Rouki,<sup>3</sup> Gérard Rudolf,<sup>1</sup> Mihai Stanoiu,<sup>3</sup> Jean-Claude Thiry<sup>1</sup>

<sup>1</sup>Institut Pluridisciplinaire Hubert Curien, CNRS/IN2P3-UdS, Strasbourg, France

<sup>2</sup>Horia Hulubei National Institute of Physics and Nuclear Engineering,  
Bucharest-Magurele, Romania

<sup>3</sup>European Commission, Joint Research Centre, Institute for  
Reference Materials and Measurements, Geel, Belgium

<sup>4</sup>Technische Universität Wien, Atominstitut der Österreichischen Universitäten, Vienna, Austria

<sup>5</sup>Nuclear Research and Consultancy Group, Petten, The Netherlands

<sup>6</sup>Universität Wien, Fakultät für Physik, Vienna, Austria

### Abstract

*Our presented research is focused on cross-section measurements of (n,xn $\gamma$ ) reactions in the framework of Generation IV nuclear reactors studies. Indeed the development of new fast reactors or the investigations concerning new fuel cycles require the improvement of nuclear databases over a wide range of energies, nuclei and reactions. One of the challenges of new measurements, in this field, is the accuracy level that they can reach and which is required by the Nuclear Data High Priority List produced by the NEA.*

*Our collaboration has developed an experimental set up based on the prompt gamma ray spectroscopy method, using the GELINA facility of IRMM at Geel (Belgium), which produces a pulsed, white neutron beam. The results concerning <sup>232</sup>Th(n,xn  $\gamma$ ) and <sup>235</sup>U(n,xn  $\gamma$ ) reactions cross-sections measurement, in the fast neutron energy domain (up to 20 MeV), are presented and compared with existing experimental data but also with theoretical TALYS calculations.*

*All these investigations are performed in the framework of ANDES program (7<sup>th</sup> framework program, EURATOM).*

## Introduction

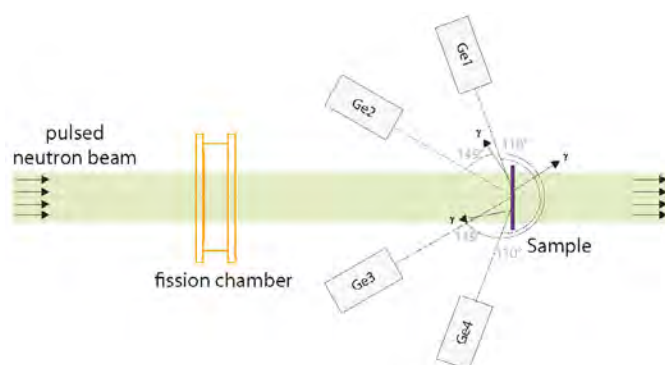
Precise knowledge of (n,xn  $\gamma$ ) reactions is a key issue in present day's reactor development studies. Indeed the new Generation IV nuclear reactors explore new energy domains, and imply reaction rates unknown or badly known at this stage. For the design of these new systems, the (n,xn) reactions have to be well described by simulation codes as they are an important energy loss mechanism and as they lead to neutron multiplication and production of radioactive isotopes. From a theoretical point of view, in the case of fissionable targets, the prediction of (n,xn) reactions implies a good knowledge of fission parameters as a strong competition exists between neutron emission and fission in the studied nuclei. Moreover (n,xn  $\gamma$ ) reactions allow to test, validate or improve theoretical codes, such as TALYS[1] (used in this work) by providing information and constraints on a wide range of nuclear structure parameters such as branching ratio, level densities, spin distributions...

The presented work is performed using the (n,xn  $\gamma$ ) technique, already used for stable isotopes as  $^{208}\text{Pb}$  [2], for which a high precision experimental setup was designed. It has already been used to measure (n,xn  $\gamma$ ) reactions on isotopes such as  $^{235}\text{U}$ ,  $^{232}\text{Th}$  and  $^{\text{nat}}\text{W}$ . In this paper, results on  $^{235}\text{U}(n,xn \gamma)$  for x=1,2, and on  $^{232}\text{Th}(n,xn \gamma)$  for x=1,2,3 are presented and compared to TALYS[1] calculations.

## Experimental setup

This section treats the applied measurement techniques as well as the experimental setup, shown in Figure 1.

**Figure 1: Sketch of the experimental setup used at GELINA, FP16/30m**



### The (n,xn $\gamma$ ) technique

This method consists in detecting the  $\gamma$  radiation from the decay of the excited nucleus created by the (n,xn) reaction using High-Purity germanium (HPGe) detectors. They yield the level population cross-section of the nucleus in a given excited state.

### The TOF technique

The experiment is realized at GELINA, a facility at IRMM, Belgium [3,4]. GELINA produces a white, pulsed neutron beam using the ( $\gamma$ ,xn) and ( $\gamma$ ,F) reactions on a depleted uranium target which leads to an incident flux spectrum from a few keV up to several MeV.

The pulsed beam enables energy separation of the incident neutrons using a time spectrum, which can be calibrated thanks to the presence of a  $\gamma$ -flash. The experimental setup is located 30 m away from the neutron source. The data acquisition resolution being 10 ns, this flight path is the best compromise between time resolution and flux intensity, allowing a resolution of 1 MeV at neutron energy of 20 MeV.

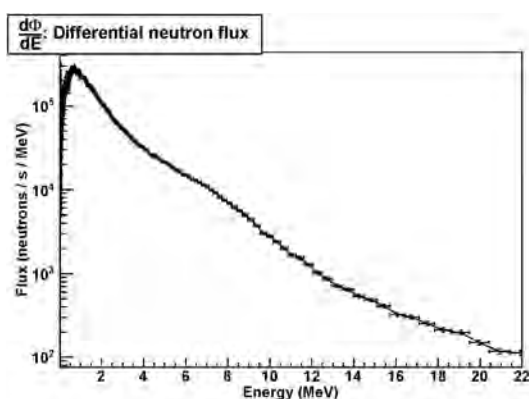
### Data acquisition

The signals arising from the detectors are processed by TNT2<sup>1</sup> cards developed at IPHC. Signals are processed online in parallel in two different channels, one determining the event time by applying the Constant Fraction Discriminator (CFD) method and one calculating the  $\gamma$ -ray energy of the incident events using the Jordanov-knoll [5,6] signal treatment method. The events are stored in list mode files, where the energy is encoded on 14 bits and the time resolution is 10 ns.

### Flux monitoring

Precision of cross-section measurements depends very strongly on the uncertainties of the incident neutron flux which is illustrated in Figure 2, thus it is of utmost importance to have very precise flux determination.

**Figure 2: Differential neutron flux measured at FP16/30m at GELINA**



The flux is measured using a <sup>235</sup>U fission chamber. The vacuum evaporated <sup>235</sup>UF<sub>4</sub> deposit is highly enriched in <sup>235</sup>U (>99.5%) and very thin (324 μg/cm<sup>2</sup> of <sup>235</sup>U). The effective thickness of the fission chamber was chosen between 6 and 7 mm, as this leads to the best ratio of fission fragment energy loss (signal) and radioactivity  $\alpha$  particle energy loss (background noise).

After extensive studies for the optimization of the fission chamber configuration and a high precision calibrating measurement performed at the Physikalisch-Technische Bundesanstalt (PTB), Braunschweig, Germany, uncertainties of 2.1% on the efficiency of the detector have been reached. See the paper of J.-C. Thiry elsewhere in these proceedings for more details.

### Gamma-ray detection

The  $\gamma$ -rays, emitted from the produced isotopes, are detected using four high purity germanium (HPGe) counters, made of planar crystals with depths ranging from 2 to 3 cm and surfaces dimensioned between 10 and 28 cm<sup>2</sup>. The detectors are optimized for high resolution detection at low energies (resolution of 0.7 keV at 122 keV). They are placed at angles of 110° and 149° which allows the angular dependence to be taken into account. Backward angles were chosen to reduce dead time caused by the observation of events due to  $\gamma$ -flash scattering.

1. TNT : Treatment for NTof.

## Data analysis

### Differential cross-sections

The differential production cross-section for a  $\gamma$  transition of interest at a given angle  $\theta_i$  and energy  $E_i$  can be expressed as:

$$\frac{d\sigma}{d\Omega}(\theta_i, E_i) = \frac{1}{4\pi} \frac{n_{GE}(\theta_i, E_i)}{n_{FC}(E_i)} \frac{\varepsilon_{FC} \sigma_{U,f}(E_i)}{\varepsilon_{GE}(E_i)} \frac{\zeta_{FC}}{\zeta_{sple}} \frac{S_{FC}}{S_{sple}} \quad (1)$$

where  $n_{GE}$  and  $n_{FC}$  represent the dead time corrected numbers of detections for a given ray in the Ge energy spectrum and for the fission chamber high energy spectrum respectively,  $\varepsilon_{GE}$  and  $\varepsilon_{FC}$  the germanium detector's and the fission chamber's efficiency,  $\sigma_{U,f}$  the  $^{235}\text{U}$  fission cross-section,  $\zeta_{FC}$  and  $\zeta_{sple}$  the areal densities of the uranium layer in the fission chamber and the sample,  $S_{FC}$  and  $S_{sple}$  the surfaces of the uranium layer in the fission chamber and the sample.

### Angle integration

The quantity of interest is the total reaction cross-section which requires integration of equation (1). One can show that the differential cross-section can be expressed as a finite sum over even degree Legendre polynomials [7,8]:

$$\frac{d\sigma}{d\Omega}(\theta) = \frac{\sigma_{tot}}{4\pi} \cdot \sum_{i=0}^{\infty} \alpha_i P_i(\cos\theta) \quad (2)$$

where  $\sigma_{tot}$  is the total angle integrated cross-section, and the  $\alpha_i$  are coefficients ( $\alpha_0 = 1$ ) depending on the angular momentum of the initial and final state  $J_i, J_f$  and the transition multipolarity  $L$  [7,8]. As the highest order Legendre polynomial in the decay distribution has order  $\leq 2L$  and  $\leq 2J_i$ , this infinite summation can be limited to  $M$  terms, where  $M = \min\{2L, 2J_i\}$ .

Usually the sum can be limited to even Legendre polynomials up to the order of 6 as the contribution of higher-order polynomials is small. Under this assumption the integrated cross-section can be obtained in very good approximation from measurements at two angles where the value of the fourth-order Legendre polynomial  $P_4$  is zero according to:

$$\sigma_{tot} \approx 4\pi \left[ w_1^* \frac{d\sigma}{d\Omega}(\theta_1^*) + w_2^* \frac{d\sigma}{d\Omega}(\theta_2^*) \right] \quad (3)$$

with  $\theta_1^* = (30.6^\circ \text{ or } 149.4^\circ)$ ,  $\theta_2^* = (70.1^\circ \text{ or } 109.9^\circ)$ ,  $w_1^* = 0.3479$  and  $w_2^* = 0.6521$  [7,8].

## Results

In this paper, the results for two different measurement sets of (n,xn  $\gamma$ ) cross-sections on  $^{235}\text{U}$  and  $^{232}\text{Th}$  are presented and compared to the prediction of the TALYS code [1].

### Samples and running time

The two samples used in these experiments have the following characteristics (see Table 1):

**Table 1: sample characteristics and measuring time**

	Purity (%)	Total mass (g)	Surface (cm <sup>2</sup> )	Thickness (mm)	Running time (h)
$^{235}\text{U}$	93.18 $\pm$ 0.031	37.43 $\pm$ 0.01	113.173 $\pm$ 0.070	0.211 $\pm$ 0.006	1248
$^{232}\text{Th}$	99.5	11.9939 $\pm$ 0.0001	36.463 $\pm$ 0.195	0.302 $\pm$ 0.004	375

## Cross-sections

Averaged cross-sections were derived from the time-of-flight spectra for neutron energy bins of suitable sizes. The integral cross-sections were summed according to Eq. (3) using the results obtained with the four HPGe detectors from both angles 110° and 149°. The cross-sections are not corrected for internal conversion. The total uncertainties vary from 5 to 7%.

Table 2 summarizes the  $\gamma$  transitions observed in various nuclei created by (n,n') and (n,2n) reactions on  $^{235}\text{U}$  and (n,n'), (n,2n) and (n,3n) reactions on  $^{232}\text{Th}$ .

**Table 2: g transitions observed corresponding to  $^{235}\text{U}(n,n')$ ,  $^{235}\text{U}(n,2n)$  and  $^{232}\text{Th}(n,n')$ ,  $^{232}\text{Th}(n,2n)$ ,  $^{232}\text{Th}(n,3n)$  reactions**

Target	Reaction	Gamma Energy (keV)	Initial level	Final level
$^{235}\text{U}$	n,n'	129.3	5/2 <sup>+</sup>	7/2 <sup>-</sup>
	n,2n	152.7	6 <sup>+</sup>	4 <sup>+</sup>
	n,2n	200.9	8 <sup>+</sup>	6 <sup>+</sup>
	n,2n	244.2	10 <sup>+</sup>	8 <sup>+</sup>

Target	Reaction	Gamma Energy (keV)	Initial level	Final level
$^{232}\text{Th}$	n,n'	49.4	2 <sup>+</sup>	0 <sup>+</sup>
	n,n'	112.75	4 <sup>+</sup>	2 <sup>+</sup>
	n,n'	171.1	6 <sup>+</sup>	4 <sup>+</sup>
	n,n'	223.7	8 <sup>+</sup>	6 <sup>+</sup>
	n,n'	550.4	5 <sup>-</sup>	6 <sup>+</sup>
	n,n'	612.3	3 <sup>-</sup>	4 <sup>+</sup>
	n,n'	665	1 <sup>-</sup>	2 <sup>+</sup>
	n,n'	714.2	1 <sup>-</sup>	0 <sup>+</sup>
	n,n'	774.1	2 <sup>+</sup>	0 <sup>+</sup>
	n,n'	681.1	0 <sup>+</sup>	2 <sup>+</sup>
	n,n'	735.9	2 <sup>+</sup>	2 <sup>+</sup>
	n,n'	780.2	3 <sup>+</sup>	2 <sup>+</sup>
	n,2n	185.7	5/2 <sup>-</sup>	5/2 <sup>+</sup>
	n,3n	182.5	6 <sup>+</sup>	4 <sup>+</sup>

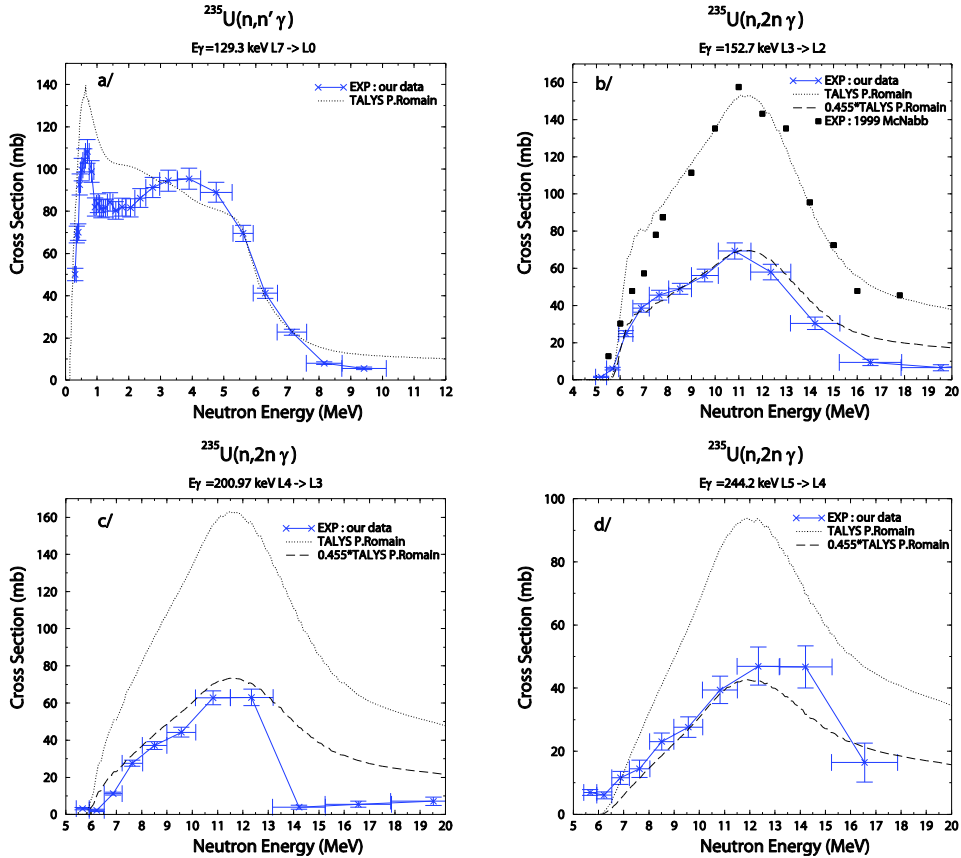
## The $^{235}\text{U}$ isotope

Figure 3 shows the results obtained for the (n,n'  $\gamma$ ) and (n,2n  $\gamma$ ) reactions on  $^{235}\text{U}$  compared to the only existing experimental data [9] and TALYS calculations [10].

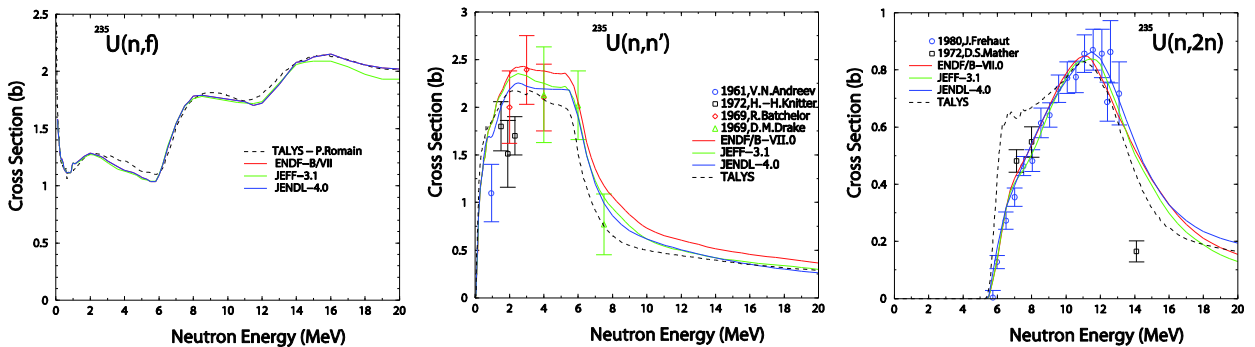
The used TALYS code was very well optimized for the fission cross-section of the isotope of interest and its descendants [10] as shown in Figure 4.

One can remark that the total cross-sections for the (n,n') and (n,2n) reactions are quite well predicted by the TALYS code. But, nevertheless, the agreement with our experimental data is not so good for (n,xn  $\gamma$ ) reactions. In the case of the 129.3 keV  $\gamma$ -transition in  $^{235}\text{U}$ , the discrepancies between experimental data and TALYS are rather small but the shape is not well reproduced in the 1 – 6 MeV neutron energy range. Concerning the (n,2n  $\gamma$ ) cross-sections, the behaviour of the experimental data is well predicted by the code but as one can see, in Figure 3 (b, c and d), a factor of 0.455 exist between theory and experiment. For the 152.7 keV  $\gamma$ -transition in  $^{235}\text{U}$  created by the  $^{235}\text{U}(n,2n)$  reaction, experimental data from [9] exist but they have been normalized to theoretical predictions by a factor whose value is not specified in the paper.

**Figure 3: Total  $\gamma$ -production cross-sections due to a/ the  $^{235}\text{U}(n,n'\gamma)$  reaction for the 129.3 keV transition (state  $5/2^+ \rightarrow 7/2^-$ ) and due to  $^{232}\text{U}(n,2n)$  reaction for the b/ the 152.7 keV transition (state  $6^+ \rightarrow 4^+$ ) c/ the 200.97 keV transition (state  $8^+ \rightarrow 6^+$ ) and d/ the 244.2 keV transition (state  $10^+ \rightarrow 8^+$ ). The results are compared to TALYS predictions and experimental data if they exist. Our data points are connected by a solid line.**



**Figure 4: TALYS total cross-section predictions for the (n,f), (n,n') and (n,2n) reactions on  $^{235}\text{U}$  compared to evaluated databases and experimental data (EXFOR)**

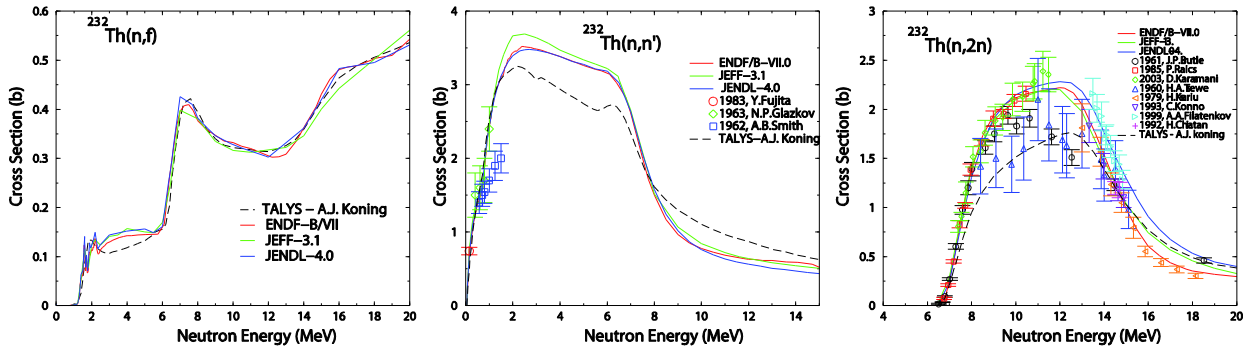




## The $^{232}\text{Th}$ isotope

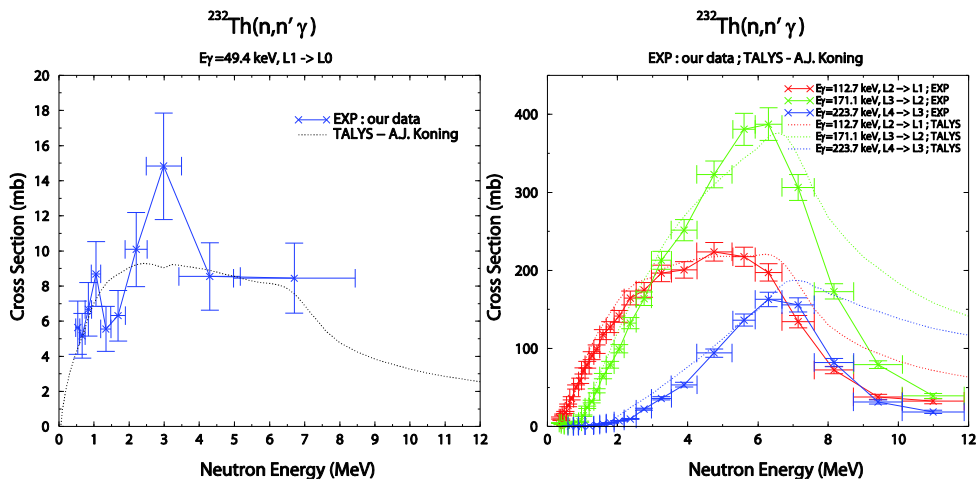
The total (n,n') reaction cross-section has been already measured in the range 0- 2 MeV while the (n,2n) reaction has been well studied as shown in Figure 5. One can see also that the TALYS calculations of the fission process in  $^{232}\text{Th}$ , made by A.J. Koning, is in good agreement with the evaluated data. On the contrary, the theoretical predictions of the total (n,n') and (n,2n) cross-sections seem to be underestimated in comparison with experimental and evaluated data.

**Figure 5: TALYS total cross-section predictions for the (n,f), (n,n') and (n,2n) reactions on  $^{232}\text{Th}$  compared to evaluated databases and experimental data (EXFOR)**



Concerning our (n,n'  $\gamma$ ) cross-section measurements, one can note in Figure 6 that the TALYS calculations are in good agreement with the experimental data except above roughly 8 MeV where the decrease of the excitation function is overestimated by the code. It has to be mentioned that the uncertainties of the 49.4 keV  $\gamma$ -transition cross-section are rather large due to the low statistic in this peak (highly converted).

**Figure 6: Total g-production cross-sections due to  $^{232}\text{Th}(n,n'\gamma)$  reaction for the 49.369 keV transition (left) (state  $2^+ \rightarrow 0^+$ ) and the 112.75 keV transition (state  $4^+ \rightarrow 2^+$ ), the 171.2 keV transition (state  $6^+ \rightarrow 4^+$ ) and the 223.6 keV transition (state  $8^+ \rightarrow 6^+$ ) (right). The results (connected by a solid line) are compared to TALYS predictions (no experimental data exist in this gamma energy range).**



Concerning higher  $\gamma$  energy transitions (Figure 7) coming from the deexcitation of the other excited bands to the states of the ground state band, the agreement between TALYS calculations and experimental data is worse than for  $\gamma$ -transitions between states belonging to the groundstate band. In this case, we were able to compare our data, in the 0 – 3 MeV neutron energy range, with existing experimental ones from [11] and the agreement is very good.

For the (n,2n  $\gamma$ ) and (n,3n  $\gamma$ ) reactions, we have, for the moment, obtained the cross-sections for the 185.7 keV  $\gamma$ -transition in  $^{231}\text{Th}$  and for the 182.5 keV  $\gamma$ -transition in  $^{230}\text{Th}$ . In the last case, the uncertainties are rather large because of the combined effect of the lower cross-sections and the low neutron incident flux (Figure 2). As for the results obtained with the  $^{235}\text{U}$  isotope, those reactions (with  $x>1$  and neutron energies higher than  $\sim 8$  MeV) are not well predicted by TALYS. More precisely, the behaviour of the excitation functions is well reproduced but for the (n,2n  $\gamma$ ) reaction the TALYS code underestimates the cross-section by a factor of 2.58 and for (n,3n  $\gamma$ ) reaction, the calculated cross-section is overestimated by a factor of 0.72.

## Discussion

These exclusive measurements are very useful to test the predictive power of theoretical calculations. As we have seen before, it is not sufficient for a model code to calculate correctly the total reaction cross-section of a process to predict with the same confidence level the  $\gamma$  production cross-sections. Indeed, the code has to take in consideration a lot of structure parameters like branching ratio, level densities, spin distributions etc... And even on an extensively studied nucleus like  $^{235}\text{U}$ , the TALYS code is not yet able to predict the (n,xn  $\gamma$ ) reaction cross-section correctly. These kinds of experimental data are thus very important and allow the improvement of the knowledge of these parameters.

There are indications that the semi-classical exciton model simply fails to properly describe the spin distribution that accompanies the pre-equilibrium process. Large deviations, in the right direction, from the exciton model are found [12,13] when a quantum-mechanical multi-step direct model is used instead of the exciton model. The correct spin dependence of the underlying DWBA cross-section is then taken into account [14], as opposed to a posteriori assigning a spin distribution to the cross-sections. It is expected that theoretical agreement will be improved if so-called FKK or other multi-step direct models are included.

## Conclusion and perspectives

After a consequent work to reduce the uncertainties of these measurements, we are currently able to measure (n,xn  $\gamma$ ) cross-sections of a precision ranging from 5 to 7%. The new data on  $^{235}\text{U}$  and  $^{232}\text{Th}$  presented in this paper, will thus complete the knowledge of  $\gamma$  production in (n,xn) reactions. These results will be subject to further investigations from experimental as well as from theoretical point of view.

In the framework of ANDES project (7<sup>th</sup> Framework program), future measurement campaigns will be devoted to the measurement of  $^{238}\text{U}$ (n,xn  $\gamma$ ) cross-sections. Indeed, some experimental data already exist but are not in agreement with each other as it can be seen in [12]. Nevertheless, with our experimental set-up, we will be able to provide cross-sections with reduced uncertainties to complete the knowledge of these reactions.

## Acknowledgements

The authors thank the team of the GELINA facility for the preparation of the neutron beam and for their strong support day after day. This work was partially supported by the Integrated Project for European Transmutation (EUROTRANS) and by the transnational access schemes Neutron data measurements at IRMM (NUDAME) and European facility for innovative reactor and transmutation data (EUFROT).

Figure 7: Total g-production cross-sections (preliminary results) due to the  $^{232}\text{Th}(n,n'\gamma)$  reaction for g-transitions from few exciting band to the ground state band compared to J.H.Dave et al. [11] and TALYS predictions. As the existing data have been measured only up to 3 MeV, the comparison is done only in this neutron energy range. Our experimental data are connected by a solid line.

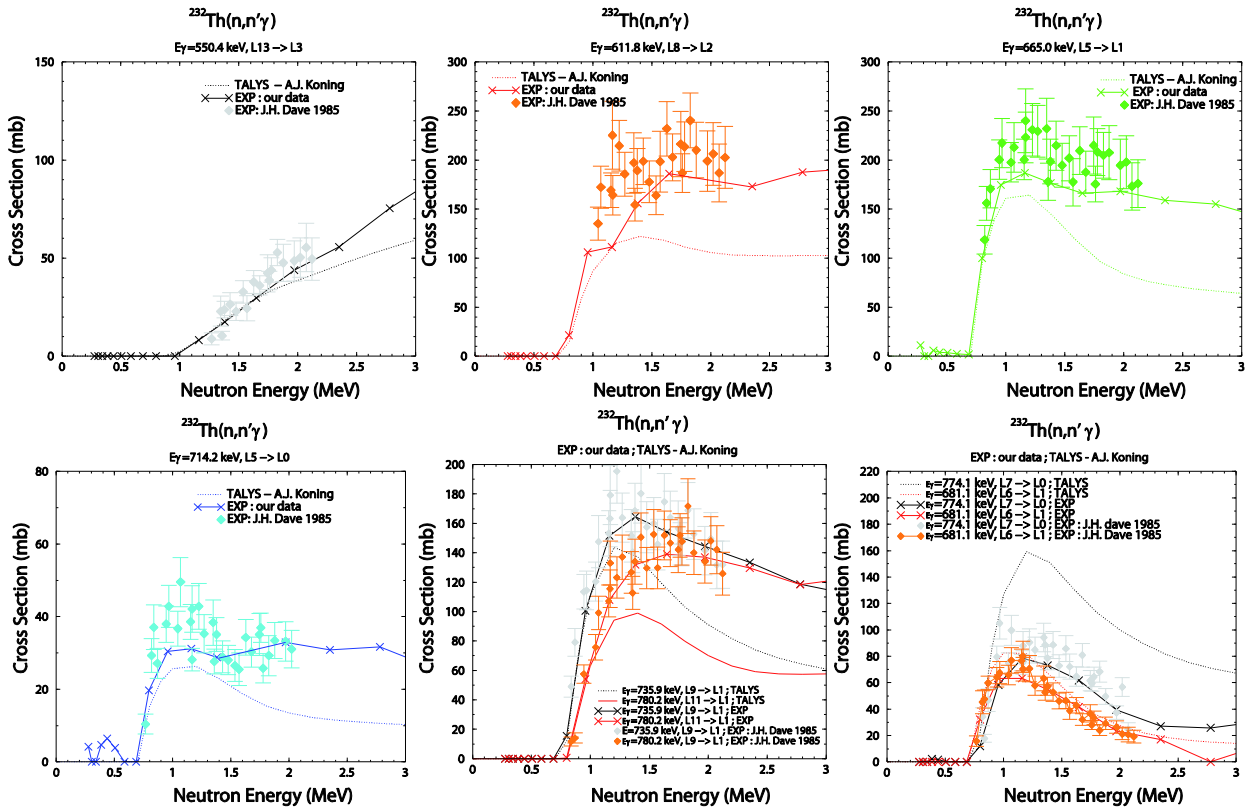
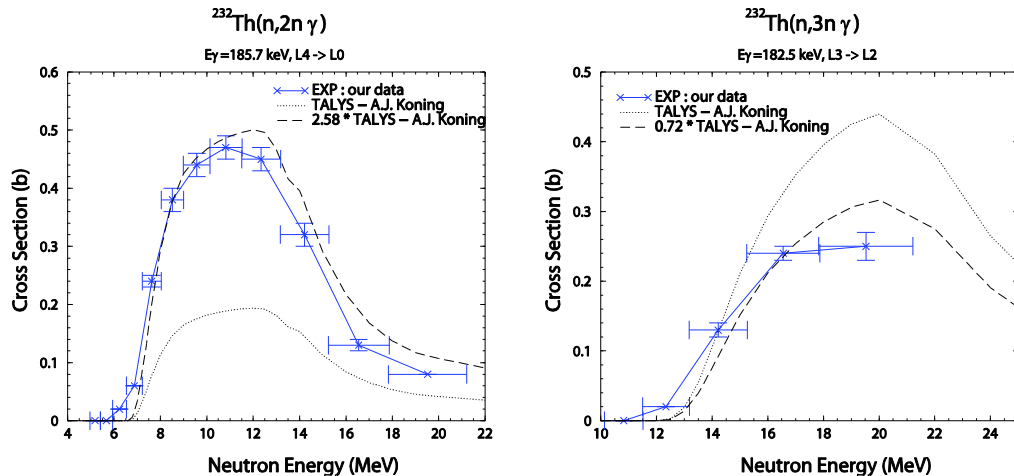


Figure 8: Total g-production cross-sections due to the  $^{232}\text{Th}(n,2n)$  reaction for the 185.7 keV transition (left) (from state  $5/2^- \rightarrow 5/2^+$ ) and due to the  $^{232}\text{Th}(n,3n)$  reaction for the 182.5 keV transition (right) (from state  $6^+ \rightarrow 4^+$ ). Our experimental data are connected by a solid line.



## References

- [1] Koning, A.J., S. Hilaire, M.C. Duijvestijn, "TALYS-1.0", *Proceedings of the International Conference on Nuclear Data for Science and Technology*, Nice, France, EDP Sciences, p. 211-214 (2008).
- [2] Mihailescu, L.C., et al., "A measurement of (n,xn  $\gamma$ ) cross-sections for  $^{208}\text{Pb}$  from threshold up to 20 MeV", *Nuclear Physics A811*, 1-27 (2008).
- [3] Tronc, D., J.M. Salomé, K. Böckhoff, "A new pulse compression system for intense relativistic electron beams", *Nuclear instruments and Methods in Physics Research A228*, 217 (1985).
- [4] Ene, D., et al., "Global characterisation of the GELINA facility for high-resolution neutron time-of-flight measurements by Monte Carlo simulations", *Nuclear instruments and Methods in Physics Research A618*, 54 (2010).
- [5] Jordanov, V.T., G.F. Knoll, "Digital synthesis of pulse shapes in real time for high resolution radiation spectroscopy", *Nuclear instruments and Methods in Physics Research A345*, 337-345 (1994).
- [6] Mihailescu, L.C., C. Borcea, A.J.M. Plompen, "Data acquisition with a fast digitizer for large volume HPGe detectors", *Nuclear Instruments and Methods in Physics Research A578*, 298 (2007).
- [7] Brune, C.R., "Gaussian quadrature applied to experimental  $\gamma$ -ray yields", *Nuclear Instruments and Methods in Physics Research A493*, 106-110 (2002).
- [8] Mihailescu, L.C., et al., "A new HPGe setup at GELINA for measurement of gamma-ray production cross-sections from inelastic neutron scattering", *Nuclear Instruments and Methods in Physics Research A531*, 375 (2004).
- [9] McNabb, D.P., et al., *Proc. of the Symposium on Capture Gamma Ray Spectroscopy*, Santa Fe, NM, USA, p.384 (1999).
- [10] Romain, P., private communication.
- [11] Dave, J.H., et al., *Nuclear Science and Engineering*, Vol.91, p.187 (1985).
- [12] Hutcheson, A., et al., *Physical Review C80*, p.014603 (2009).
- [13] Kawano, T., P. Talou, M.B. Chadwick, *Nuclear Instruments and Methods in Physics research A562*, 774 (2006).
- [14] Koning, A.J., M.B. Chadwick, *Physical Review C56*, p.970 (1997).

## Fission studies in the renovated IGISOL facility

H. Penttilä, T. Eronen, D. Gorelov, J. Hakala, A. Jokinen, A. Kankainen, P. Karvonen, V. Kolhinen, I.D. Moore, M. Reponen, J. Rissanen, A. Saastamoinen, V. Sonnenschein, J. Äystö  
Department of Physics, University of Jyväskylä, Finland

### Abstract

Particle induced fission has been utilised in the IGISOL (Ion Guide Isotope Separator On-Line) facility in the Accelerator Laboratory of the University of Jyväskylä, JYFL, since 1980's to study the nuclear structure of neutron rich nuclei [1]. The ion guide technique allows the production of mass separated ion beams of any element, enabling the possibility to perform systematic studies. The primary motivation of such studies has been the basic nuclear structure research. However, the properties of the ion guide technique make the facility suitable for measuring nuclear data required e.g. for the development of nuclear energy production applications. Such data include atomic masses [2,3], independent fission yield distributions [4], delayed neutron probabilities [5] and beta decay heat [6]. The examples show that usually the nuclear data measurements for applications and the basic research go together and the same experiments benefit the both goals of research.

The IGISOL facility is currently (as October 2010) moving to a new location next to the recently installed high current MCC30/15 light-ion cyclotron [7]. In the same instance, the facility will have a major upgrade. The improvements include more effective beam transportation in the experimental area, better access with laser beams to the target area and the other stages of ion path, as well as designated beam lines for test ion sources. To fully utilise the intense proton and deuteron beams available from the new accelerator, a program to build a neutron converter target has been initiated. A converter target would allow studies with fast neutron-induced fission, which has certain benefits over charged particle-induced fission as a production reaction for the most neutron rich species. Improved access to more neutron rich nuclei would boost basic nuclear structure research, and in particular, the neutron production allows determine the independent fission yields of key actinides in a simulated fast reactor neutron field. This program is intended to take place in collaboration with Uppsala University.

The new IGISOL facility is intended to be operational again in the beginning of 2011.

## The IGISOL facility

The IGISOL facility [8] consists of a multitude of instruments for ion manipulation. The main devices are a magnetic mass separator based on the ion guide technique [1]; a RFQ cooler trap [9] that can be used not only for cooling and bunching the ion beam but also storing and optical pumping [11,12] of the ions; a double Penning trap system known as JYFLTRAP [12]; a laser ion source FURIOS [13] as well as a collinear ion (or atom) laser spectroscopy set-up [14], run by the Manchester and Birmingham universities.

The ion guide technique is based on stopping the primary ions from nuclear reactions in noble gas, typically in helium. Because of the high ionization potential of the buffer gas, the stopped species are preserved as ions long enough to be evacuated from the stopping volume still as ions. In the original ion guide method in the mid-1980's in the University of Jyväskylä the ions are evacuated entirely by gas flow, which limits the stopping volume in practice to a few 100 cm<sup>3</sup> at most. In fission and in heavy ion induced fusion reactions the reaction products are too energetic to be efficiently stopped in such a small volume. The volume of the gas cell can be increased, if voltages are applied inside the ion guide to drift the ions through the gas [15-19]. The larger gas cell is capable to stop more ions. On the other hand, the larger gas cells seem also to be more sensitive to the practically unavoidable ionization of the buffer gas [20].

At the IGISOL facility, ions are extracted from helium using a differential pumping system and mass separated using a dipole magnet with a mass resolving power (MRP) of about 500. This is adequate to select an isobar – species with the same mass number  $A$  – to be sent directly to subsequent spectroscopy, or to JYFLTRAP [12] for more refined purification. In a typical experiment the ions are first collected in a radiofrequency quadrupole preparation trap, RFQ. At this stage, the energy staggering of the mass selected ion beam is removed by applying buffer gas cooling. The continuous beam from the mass separator is also compressed to short ion bunches. This is necessary for the operation of JYFLTRAP, since a Penning trap deals with ion bunches. Bunching the beam also significantly reduces the background in the collinear laser spectroscopy, because the photon detection can be gated by the arrival of the ion bunch in the laser interaction region [14]. Furthermore, the ions stored in the RFQ can be optically pumped with lasers to an appropriate atomic state for spectroscopy [11,12].

The purification or mass separation achieved with JYFLTRAP is sufficient to separate the different species within the isobar, resulting in truly monoisotopic beams of the studied species. The MRP of this separation can in many cases exceed  $10^5$  [4]. Beta, gamma, and beta delayed neutron decay studies significantly benefit from such sources and a vivid research program is established around the decay studies of the purified sources.

Even more refine purification can be achieved by using so-called Ramsey-cleaning technique. An ultimate example is the separation of  $^{133m}\text{Xe}$  from the  $^{133}\text{Xe}$  ground state by their different mass. The mass difference is 300 keV/c<sup>2</sup> or 1.7 ppm. It is worth noting that it is not question of only identifying the different species but physically separating and producing a sample consisting of solely of  $^{133m}\text{Xe}$  species. The size of these samples is of the order of  $10^6$  atoms and they are needed for the Comprehensive Nuclear Test Ban Treaty Organisation CTBTO detector network calibrations. This achievement is described in detail in [21].

In addition to beam purification, JYFLTRAP can be used as an instrument to determine atomic masses very precisely [2]. Atomic masses of over 200 neutron-rich nuclei have been measured with JYFLTRAP with an accuracy of a few keV [3].

## Fission based studies at the IGISOL facility

At the IGISOL facility the particle induced fission of natural uranium and thorium targets has since the 1980's been used to produce neutron rich isotopes for nuclear spectroscopy studies. During these research more than 30 new neutron rich isotopes has been discovered along the systematic studies of shell structure evolution in particular in neutron rich between Zr and Cd ( $Z = 40 - 48$ ). The systematic studies of the nuclear shape evolution using the collinear laser spectroscopy in the same proton region have often been extended to the proton rich side of the valley of the beta stability, since the beams of any of these refractory elements have been available nowhere else. The precise

atomic mass studies with JYFLTRAP in the same mass region have revealed a correspondence between the nuclear shape and the atomic mass. It was also found that the evaluated atomic masses of neutron rich nuclei can in many cases be more than 1 MeV/c<sup>2</sup> off from the measured values [22].

### **Fission studies for nuclear data - ANDES**

The monoisotopic samples of fission products available after Penning trap purification are ideal for studies with a Total Absorption Spectrometer (TAS). These studies give information of the reactor decay heat [23]. The samples produced with JYFLTRAP are free from the isobaric background other than produced by the decay of the sample itself. In cases where the mass difference between the isomer in the ground state is a few hundred keV, it is even possible to achieve isomeric purification. In recent years, practically all the experiments defined as “requested TAS measurements” by OECD Nuclear Energy Agency [23] have taken place at IGISOL [6,24].

Measurements of beta delayed neutron probabilities have been performed at IGISOL already in 1990’s [25] and again in late 2000’s [5]. These measurements are also related to the detector development for the Low Energy Branch experiments at the Super Fragment Separator (SFRS) in the future FAIR facility. The very last measurement utilising fission reaction at the IGISOL facility before it was taken down to be moved to a new location was indeed a beta delayed neutron experiment within the ANDES collaboration utilising the newly developed BELEN detector [5].

### **Fission yield studies**

Both the decay heat measurements and the delayed neutron experiments are important for the design of the advanced nuclear reactors. Another important data for the design are the independent fission yields.

The chemical unselectivity of the ion guide technique makes it also an attractive approach to study the fission yield distributions. Due to the ion production mechanism of IGISOL only directly produced ions are mass separated and hence independent fission product yields can be measured. An extensive effort in this field has been taken place in Tohoku University [26-28] utilising the ion guide or IGISOL technique adapted to their facility already at late 1980’s [29]. Some fission yield experiments have been performed in Jyväskylä as well using the means of gamma spectroscopy, but a real breakthrough was the utilization of the Penning trap for the determination of fission yields. The method is based on the unambiguous identification of most of the fission products – including even some isomers – by their mass. The quantification of the mass separated fission products is based on ion counting after the Penning trap, which makes the technique also extremely sensitive.

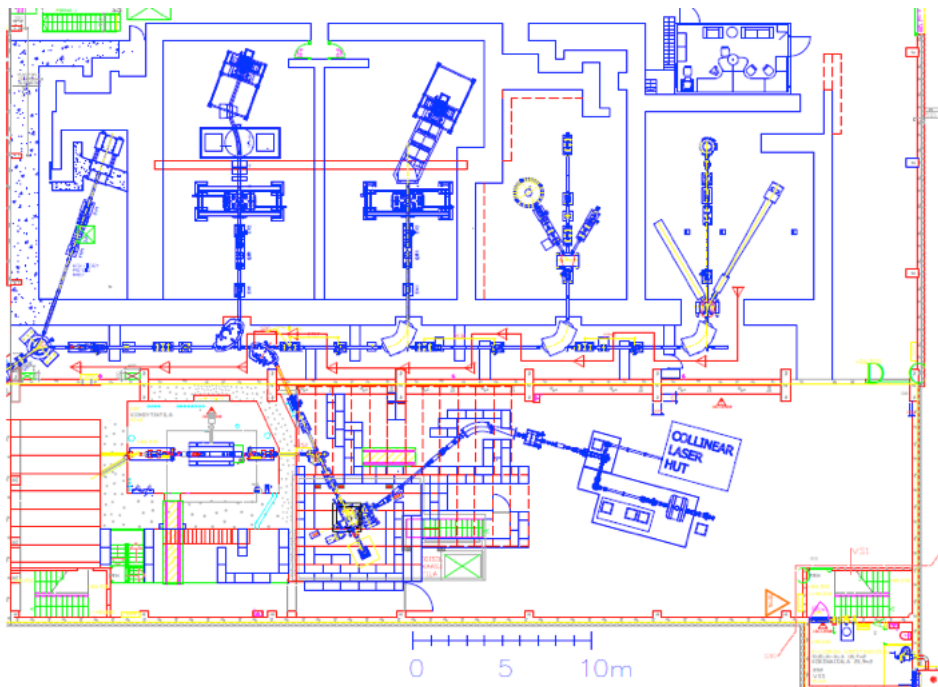
The method was tested with 25 MeV and 50 MeV proton-induced fission of <sup>238</sup>U. The data are internally reproducible and the results for Rb and Cs yields in the 50 MeV proton-induced fission agree with previous measurements. More details can be found in [4].

A much more complete set of yield distributions in 25 MeV proton induced fission of <sup>238</sup>U than just Rb and Cs was measured. The preliminary yields were given in a report of the EURISOL project [30]. Since then, the data has been thoroughly reanalysed. An article of this data is in preparation. In addition, the yield distribution of 25 MeV proton-induced fission of <sup>232</sup>Th, and the yields for selected elements in 25 MeV deuteron-induced fission of <sup>238</sup>U were measured and currently in analysed.

### **The extended IGISOL facility – IGISOL 4**

The IGISOL facility is currently (as October 2010) being moved to new premises within the Accelerator Laboratory of the University of Jyväskylä. This will be the third location of the facility, and including the major upgrade the facility experienced in the early 2000’s, this will be the fourth version of the facility, IGISOL 4. The new location in the experimental hall extension provides several improvements, including more effective beam transportation in the experimental area, better access to the target area with the laser beams, lines for test ion sources for tuning and calibration of the experimental equipment. The best way to benefit from the intense light ion beams available from the new MCC30/15 cyclotron is foreseen to convert it to neutron beams to be used for particle induced fission.

**Figure 1: The accelerator laboratory of the Department of Physics, University of Jyväskylä (JYFL) as expected in the near future. The K-130 heavy ion cyclotron will be devoted mainly for heavy ion research, while the new MCC30/15 light ion cyclotron serves experiments using 18 – 30 MeV protons or 9 – 15 MeV deuterons. The main user of such beams, the extended IGISOL facility, will be moved next to MCC30/15. The move of IGISOL allows some rearrangement of the old laboratory. The currently expected arrangement is shown in the figure.**



### **Beam distribution system**

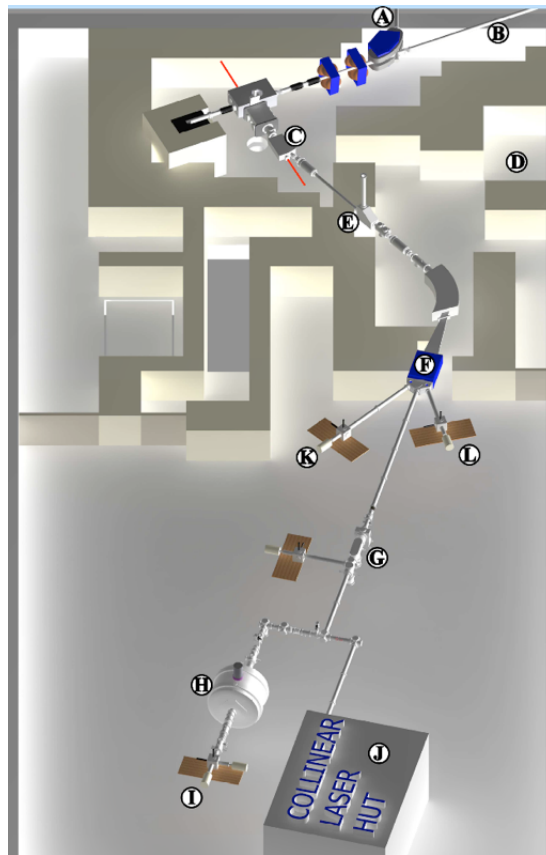
The layout design of new measurement area has been strongly focused to the operation of JYFLTRAP, which is involved to the majority of IGISOL experiments. Due to increased distances between the switchyard, the RFQ and the trap, also the better positioning for the beam diagnostic units is possible and the tuning of the beam transportation between these devices will be improved. An increased space after the trap makes it possible to build more sophisticated and complex detector setups. In the new layout, the RFQ is located at the central line, at the optical axis of the dipole magnet exit. This provides the best ion optics for mass separated beams to be injected to the RFQ, where the cooled and bunched beams are transported further to the collinear laser spectroscopy setup or to JYFLTRAP.

The collinear laser spectroscopy facility will be moved from the upstairs to the main floor of the IGISOL facility. The beam transfer line from the RFQ to the laser hut becomes shorter and the visibility to the optical axis of the RFQ makes it possible to perform the laser spectroscopy directly inside the RFQ. For the laser spectroscopy studies, the RFQ and the trap will be electrically isolated from each other. In this way, JYFLTRAP can be operated also during the laser experiments. It is also possible to use the superior ion species identification of the trap by the ion mass in a connection of the laser experiments. This would greatly benefit especially the experiments utilizing the in-RFQ laser spectroscopy.

A more advanced beam distribution is also allowed by a new switchyard system, which will be redesigned in order to allow the fast switching between three beam lines. This would provide the possibility for on-line beam monitoring during the beam pulsing cycles of trap experiments. Unlike in the present IGISOL facility, all beam lines from the switchyard will be fully accessible. This allows the building of permanent beam monitoring setup to one side beam line while another side beam line can be reserved for temporary decay spectroscopy experiments. The possibility for



Figure 2: The extended IGISOL facility: A) Beam line from MCC30/15. B) Beam line from K130. C) The 15-degree bend. D) Storage for active material. E) The 90-degree bend for external ion source. F) Switchyard. G) RFQ cooler and trap. H) JYFLTRAP Penning trap. I) Post-trap experimental area. J) Laser hut. K, L) Permanent experimental and monitoring stations.



simultaneous distribution of different masses to the separate beam lines is also investigated. This would allow the trap and decay spectroscopy experiments of similar mass range to be executed simultaneously.

### **IGISOL front-end design**

The intensive light ion beams provided by the new MCC30/15 cyclotron make it necessary to redesign the present ion guides to fully benefit the beam intensities available. Heat transfer simulations show that at  $80 \mu\text{A}$  beam current of 30 MeV protons the target temperature exceeds the melting point of uranium. The performance of the present fission ion guide has not been systematically investigated further than up to  $10 \mu\text{A}$  proton beam current. The bottleneck however was not the front end but the radiation level in the switchyard of the mass separator system, located in the experimental area, which prevented further increase of proton beam intensity. The full benefit of the high intense light ion beams can be reached with neutron converter targets that would allow the use of neutron-induced fission reactions. The converter target is planned to be built in collaboration with Uppsala University.

The severest limitation of the fission ion guide used at IGISOL is the stopping efficiency. The survival efficiency of the stopped ions is determined to be about 6% while the stopping efficiency is estimated to be of the order of  $10^{-4}$ . The simulations agree with the estimated stopping efficiency; they also show that all fission fragments are stopped within a 300 mm radius from the target. Thus, a fission ion guide with a cylindrical symmetry and approximately 400 mm long, 400 mm in

diameter would increase the stopping efficiency three orders of magnitude. Such a large gas cell naturally cannot any more operate with the buffer gas flow alone, but a voltage grid is needed to transport the ions to the exit nozzle of the stopping gas cell, similarly to *e.g.* the CARIBU ion source in the Argonne National Laboratory [15,31]. An even more advantaged option is to use a cryogenic ion guide, where the stopping gas temperature is lowered to a few tens Kelvin. A full-scale prototype of such a device for the future heavy ion beam facility FAIR (Facility for Antiproton and Ion Research) has been tested off-line in KVI, Groningen. In the first tests the stopped radioactive recoil ions from an internal alpha source have been transported from a distance of about 1 meter to the exit nozzle and successfully extracted with an efficiency of about 2% [32].

The current plan at the IGISOL facility is to rebuild the facility based on small volume ion guides to be able to compare the yields to the previous installation. However, there is a space reservation in the new IGISOL facility front end for a big enough target chamber to house a large gas cell along with a neutron converter target, whose benefits will be discussed below. The large gas cell is intended to be built within about one or two years from the first successful on-line runs in the new laboratory.

Beams from the present K-130 cyclotron will also be available at the new IGISOL 4 laboratory after the upgrade. The heavy ion induced reactions as well as light particle induced reactions with equally wide range of projectile energies can still be studied as before the upgrade. Since IGISOL is the main user of light ion beams at JYFL and the major fraction of the IGISOL experiments is focused to the light ion induced reactions, an expected annual beam time of the IGISOL facility is extended to 4000 hours.

In the upgrade, the laser light paths for the LIS (laser ion source) and LIST (laser ion source trap) to the IGISOL target area will be improved. A 15-degree electrical beam bender located just after the extractor chamber provides a direct sight to the optical axis of the SPIG [33] electrode. A similar arrangement for the LIS method from the backside of the ion guide has also been designed. For both paths the laser beams enter the target area from the top through narrow channels, bend with mirrors through a maze to ensure the radiation protection. The radiation safety issues in general have played a critical role in the new IGISOL cave area design. Since the access to the IGISOL target area is often restricted a long time after the target irradiation, a specified ion guide preparation area has been included to the new layout to make the preparation of the further experiments easier. This area is located outside the target area, but it is still inside the radiation shielding.

The present vacuum pumps will be recycled to the new facility. The roots pump cluster used to evacuate the target chamber will be made oil free by installing a new oil free backing pump. In addition to providing as oil-vapour free operation as possible for the ion guides, which is a necessity for their proper performance, the oil-free pumping of ion guide buffer gas will allow helium to be recycled also during the fission experiments by using a closed helium cycle, in which the helium is purified and reused locally inside the radiation shielding.

### **Prospects of neutron induced fission**

High intense light ion beams can be utilised by using neutron converter target. The conversion rate is relatively low: only a few percent can be expected even in the best case. In addition, while the pencil-like proton beam can be impinged to a target of 10 mm in diameter, produced neutron beam is wider, diverse and subject of severe backscattering. This can partly be compensated by that the fission ion guide probably never will be capable of taking more than 30 – 40  $\mu\text{A}$  of proton beam, while it is realistic though challenging to expect about 200  $\mu\text{A}$  protons to be impinged in the converter target. In addition, the use of neutrons has other benefits.

From the point of view deducing the fission yields for reactions relevant for simulating the processes in the advantaged nuclear power plants, the use of neutron-induced fission is self-explanatory. The other goal of the fission ion guide and the IGISOL facility developments is to use fission to produce neutron rich nuclei even further from stability for basic nuclear structure research. Also the latter goal can benefit from the possibility to use neutron-induced fission.

Using neutron induced fission gives additional freedom to the design of fission ion guide. The ionisation of the buffer gas reduces the performance of the ion guide. Unlike the charged particles, neutrons do not ionise the stopping gas. The fission target can thus be placed in the stopping gas volume, while in the case of proton-induced fission, the proton beam and therefore also the target

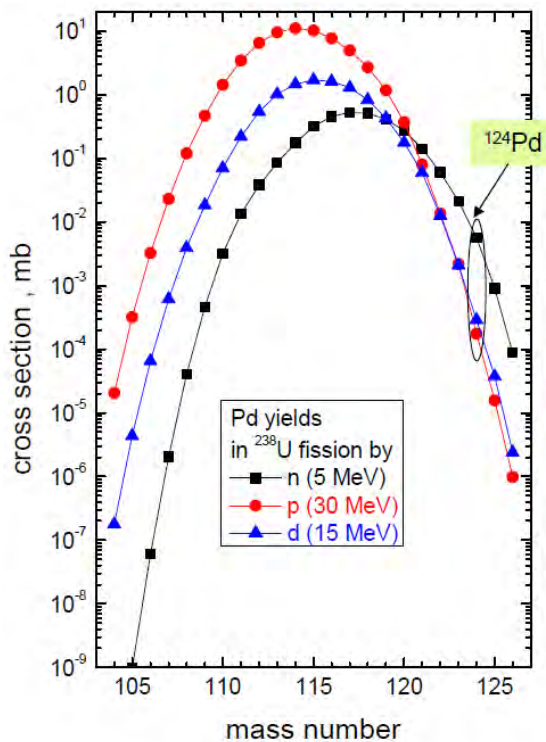
must be separated from the stopping volume. This means that in the case of proton induced fission, only a relatively narrow cone of all fission fragments can enter the stopping volume in the first place. The gain in this geometrical factor is more than 5.

Figure 3 shows the calculated fission yield distributions for palladium isotopes in 30 MeV proton-, 15 MeV deuteron- and 5 MeV neutron induced fission. The yield of the most neutron-rich isotopes is orders of magnitude higher in neutron-induced fission. Furthermore, as shown in Figure 4 for  $A = 118$  isobar, the yield of the isotopes closer to stability neutron induced fission is orders of magnitude less than in proton induced fission. This helps avoiding another bottleneck: the space charge limit of the purification Penning trap. The charge of the collected ions in the Penning trap influences in its operation, and even when the trap can tolerate the total charge, the fraction of the ions to be purified should not be less than  $10^{-4}$ .

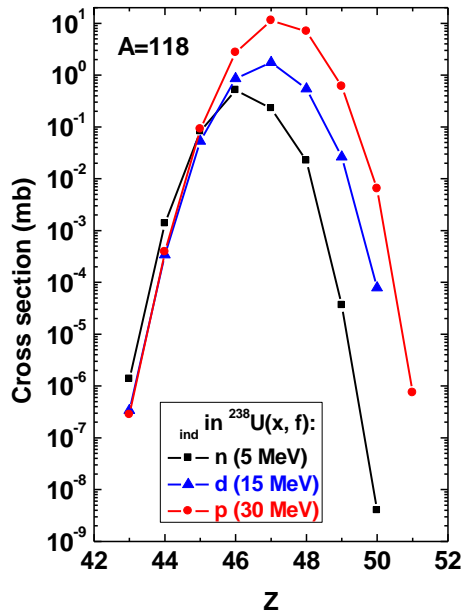
Adding up five times more primary proton beam, a geometrical factor of 5, and 50 times higher production cross-section (for  $^{124}\text{Pd}$  highlighted as an example in Figure 3) gives a compensation factor more than 1000 to recover from the beam intensity losses in the neutron conversion. Thus, with neutron-induced fission the most neutron-rich isotopes can be produced at about the same rate as in proton induced fission, however, with much less isobaric background.

Already a very low rate of ions is sufficient for the atomic mass measurements utilising JYFLTRAP. In an optimal atomic mass measurement with a Penning trap, the fraction of ion bunches with exactly one ion in the precision (or the mass measurement) trap at the time should be as large as possible. Typically, the manipulation of each ion bunch takes 150 – 400 ms, and therefore the optimal rate of ions is just a few ions per second. For gamma- and beta ray spectroscopy a yield of at least several tens of isotopes per second is necessary.

**Figure 3: Calculated production cross-sections for Pd isotopes in the fission of  $^{238}\text{U}$  induced by neutrons, protons and deuterium nuclei**



**Figure 4: Calculated independent nuclear charge distributions for A = 118 isobar in the fission of  $^{238}\text{U}$  induced by neutrons, protons and deuterium nuclei. Note that neutron rich nuclei in this figure are in the left.**



## Conclusions

Though in the IGISOL move to a new location the immediate upgrades are largely focused to the facility downstream from the front-end, there is at least one major improvement of the IGISOL front end on the way. In order to get a full benefit from the high intense light ion beams provided by the new MCC30/15 cyclotron, a neutron converter target will be designed. The neutrons will be used to induce fission in actinide targets. In addition, the LIS and the LIST methods will clearly benefit from the better access to the optical axis of the ion guide with laser beams. The first experiments in the renovated laboratory are expected to take place in summer 2011.

## Acknowledgements

This work is supported by the Academy of Finland under the Finnish Centre of Excellence Programme 2006-2011 (Project No. 213503, Nuclear and Accelerator Based Physics Programme at JYFL).

## References

- [1] Äystö, J., “Development and applications of the IGISOL technique”, *Nucl. Phys.*, A 693, 477 (2001).
- [2] Jokinen, A., et al., “Precision experiments on exotic nuclei at IGISOL”, *Int. J. Mass Spectrometry*, 251,204 (2006).
- [3] [http://research.jyu.fi/igisol/JYFLTRAP\\_masses/index.php](http://research.jyu.fi/igisol/JYFLTRAP_masses/index.php).
- [4] Penttilä, H., et al., “Determining the isotopic fission yield distributions by a Penning trap”, *Eur. Phys. J.*, A 44, 124 (2010).
- [5] Gomez-Hornillos, M.B., et al., “First Measurements with the BEta deLayEd Neutron Detector (BELEN-20) at the JYFL Penning Trap”, *proceedings of the International Nuclear Physics Conference (INPC 2010)*, July 4 – 9, 2010, to be published in *Journal of Physics: Conference Series*, (2011).
- [6] Algora, A., et al., “Reactor decay heat in  $^{239}\text{Pu}$ : Solving the gamma discrepancy in the 4-3000 s cooling period”, *Phys. Rev. Lett.*, accepted for publication (2010).
- [7] [www.jyu.fi/fysiikka/en/research/accelerator/accelerator/index\\_html/mcc30](http://www.jyu.fi/fysiikka/en/research/accelerator/accelerator/index_html/mcc30).
- [8] Karvonen, P., et al., “Upgrade and yields of the IGISOL facility”, *Nucl. Instr. and Meth.*, B 266, 4454 (2008).
- [9] Nieminen, A., et al., “Beam cooler for low-energy radioactive ions”, *Nucl. Instr. and Meth.*, A 469, 244 (2001).
- [10] Kolhinen, V., et al., “JYFLTRAP: A Cylindrical Penning Trap for Isobaric Beam Purification at IGISOL”, *Nucl. Instr. and Meth.*, A 528, 776 (2004).
- [11] Cheal, B., et al., “Laser pumping of ions in a cooler buncher”, *Hyp. Int.*, 181, 107 (2008).
- [12] Cheal, B., et al., “Laser Spectroscopy of Niobium Fission Fragments: First Use of Optical Pumping in an Ion Beam Cooler”, *Phys. Rev. Lett.*, 102, 222501 (2009).
- [13] Moore, I. D., et al., “Development of a laser ion source at IGISOL”, *Phys.*, G 31, S1499-S1502 (2005).
- [14] Campbell, P., et al., “Laser Spectroscopy of Cooled Zirconium Fission Fragments”, *Phys. Rev. Lett.*, 89, 082501 (2002).
- [15] Savard, G., et al., “Development and operation of gas catchers to thermalize fusion–evaporation and fragmentation products”, *Nucl. Instr. and Meth.*, B 204, 582 (2003).
- [16] Wada, M., et al., “Slow RI-beams from projectile fragment separators”, *Nucl. Instr. and Meth.*, B 204, 570 (2003).
- [17] Weissman, L., “Conversion of 92 MeV/u  $^{38}\text{Ca}/^{37}\text{K}$  projectile fragments into thermalized ion beams”, *Nucl. Instr. and Meth.*, A 540, 245 (2005).
- [18] Neumayr, J. B., et al., “The ion-catcher device for SHIPTRAP”, *Nucl. Instr. and Meth.*, B 244, 489 (2006).
- [19] Petrick, M., et al., “Online test of the FRS Ion Catcher at GSI”, *Nucl. Instr. and Meth.*, B 266, 4493 (2008).
- [20] Moore, I. D., et al., “New concepts for the ion guide technique”, *Nucl. Instr. and Meth.*, B 266, 4334 (2008).
- [21] Peräjärvi, K., et al., “Ultra-high resolution mass separator - Application to detection of nuclear weapons tests”, *Applied Radiation and Isotopes*, 68, 450 (2010).

- [22] Hager, U., et al., "First Precision Mass Measurements of Refractory Fission Fragments", *Phys. Rev. Lett.*, 96, 042504 (2006).
- [23] Nuclear Energy Agency (NEA), "Assessment of Fission Product Decay Data for Decay Heat Calculations", *International Evaluation Co-operation*, Vol. 25, NEA/WPEC-25, OECD/NEA, Paris (2007).
- [24] Nichols, A.L., C. Nordborg, *Total Absorption Gamma-ray Spectroscopy (TAGS), Current Status of Measurement Programmes for Decay Heat Calculation and Other Applications*, Report INDC(NDS)-0551, IAEA NDC, Vienna (2009).
- [25] Mehren, T., et al., "Beta-decay half-lives and neutron-emission probabilities of very neutron-rich Y to Tc isotopes", *Phys. Rev. Lett.*, 77, 458 (1996).
- [26] Kudo, H., et al., "Most probable charge of fission products in 24 MeV proton induced fission of  $^{238}\text{U}$ ", *Phys. Rev. C* 57, 178 (1998).
- [27] Goto, S., et al., "Isomeric yield ratios of fission products in proton-induced fission of  $^{232}\text{Th}$ ", *J. Radioanal. Nucl. Chem.*, 239, 109 (1999).
- [28] Kaji, D., et al., "Most Probable Charge of Fission Products in Proton-Induced Fission of  $^{238}\text{U}$  and  $^{232}\text{Th}$ " *Journal of Nuclear and Radiochemical Sciences*, Vol.3, No.2, 7 (2002).
- [29] Yoshii, M., et al., "The ion-guide isotope separator on-line at the Tohoku University Cyclotron", *Nucl. Instr. and Meth.*, B 26, 410 (1987).
- [30] [www.eurisol.org/site02/index.php](http://www.eurisol.org/site02/index.php).
- [31] Savard, G., et al., "Radioactive beams from gas catchers: The CARIBU facility", *Nucl. Instr. and Meth.*, B 266, 4086 (2008).
- [32] Dendooven, P., private communication.
- [33] Karvonen, P., et al., "A sextupole ion beam guide to improve the efficiency and beam quality at IGISOL", *Nucl. Instr. and Meth.*, B 266, 4794 (2008).

## Neutron-induced fission cross-section of $^{233}\text{U}$ , $^{241}\text{Am}$ and $^{243}\text{Am}$ in the energy range $0.5 \text{ MeV} \leq E_n \leq 20 \text{ MeV}$

F. Belloni,<sup>1,2</sup> P. M. Milazzo,<sup>1</sup> M. Calviani,<sup>3,4</sup> N. Colonna,<sup>5</sup> P. Mastinu,<sup>3</sup> U. Abbondanno,<sup>1</sup> G. Aerts,<sup>2</sup> H. Álvarez,<sup>6</sup> F. Álvarez-Velarde,<sup>7</sup> S. Andriamonje,<sup>2</sup> J. Andrzejewski,<sup>8</sup> L. Audouin,<sup>9</sup> G. Badurek,<sup>10</sup> P. Baumann,<sup>11</sup> F. Bečvář,<sup>12</sup> E. Berthoumieux,<sup>2</sup> F. Calviño,<sup>13</sup> D. Cano-Ott,<sup>7</sup> R. Capote,<sup>14,15</sup> C. Carrapiço,<sup>16</sup> P. Cennini,<sup>4</sup> V. Chepel,<sup>17</sup> E. Chiaveri,<sup>4</sup> G. Cortes,<sup>13</sup> A. Couture,<sup>18</sup> J. Cox,<sup>18</sup> M. Dahlfors,<sup>4</sup> S. David,<sup>9</sup> I. Dillmann,<sup>19</sup> C. Domingo-Pardo,<sup>19,20</sup> W. Dridi,<sup>2</sup> I. Duran,<sup>6</sup> C. Eleftheriadis,<sup>21</sup> M. Embid-Segura,<sup>7</sup> L. Ferrant†,<sup>9</sup> A. Ferrari,<sup>4</sup> R. Ferreira-Marques,<sup>17</sup> K. Fujii,<sup>1</sup> W. Furman,<sup>22</sup> I. Goncalves,<sup>17</sup> E. González-Romero,<sup>7</sup> A. Goverdovski,<sup>23</sup> F. Gramegna,<sup>3</sup> C. Guerrero,<sup>7,4</sup> F. Gunsing,<sup>2</sup> B. Haas,<sup>24</sup> R. Haight,<sup>25</sup> M. Heil,<sup>19</sup> A. Herrera-Martinez,<sup>4</sup> M. Igashira,<sup>26</sup> E. Jericha,<sup>10</sup> F. Käppeler,<sup>19</sup> Y. Kadi,<sup>4</sup> D. Karadimos,<sup>27</sup> D. Karamanis,<sup>27</sup> M. Kerveno,<sup>11</sup> P. Koehler,<sup>28</sup> E. Kossionides,<sup>29</sup> M. Krčička,<sup>12</sup> C. Lamboudis,<sup>21</sup> H. Leeb,<sup>10</sup> A. Lindote,<sup>17</sup> I. Lopes,<sup>17</sup> M. Lozano,<sup>15</sup> S. Lukic,<sup>11</sup> J. Marganec,<sup>8</sup> S. Marrone,<sup>5</sup> T. Martínez,<sup>7</sup> C. Massimi,<sup>30</sup> A. Mengoni,<sup>4,14</sup> C. Moreau,<sup>1</sup> M. Mosconi,<sup>19</sup> F. Neves,<sup>17</sup> H. Oberhummer,<sup>10</sup> S. O'Brien,<sup>18</sup> J. Pancin,<sup>2</sup> C. Papachristodoulou,<sup>27</sup> C. Papadopoulos,<sup>31</sup> C. Paradela,<sup>6</sup> N. Patronis,<sup>27</sup> A. Pavlik,<sup>32</sup> P. Pavlopoulos,<sup>33</sup> L. Perrot,<sup>2</sup> M. T. Pigni,<sup>10</sup> R. Plag,<sup>19</sup> A. Plompen,<sup>34</sup> A. Plukis,<sup>2</sup> A. Poch,<sup>13</sup> J. Praena,<sup>15</sup> C. Pretel,<sup>13</sup> J. Quesada,<sup>15</sup> T. Rauscher,<sup>35</sup> R. Reifarth,<sup>25</sup> M. Rosetti,<sup>36</sup> C. Rubbia,<sup>37</sup> G. Tagliente,<sup>13</sup> P. Rullhusen,<sup>34</sup> J. Salgado,<sup>16</sup> C. Santos,<sup>16</sup> L. Sarchiapone,<sup>4</sup> I. Savvidis,<sup>21</sup> C. Stephan,<sup>9</sup> G. Tagliente,<sup>5</sup> J. L. Tain,<sup>20</sup> L. Tassan-Got,<sup>9</sup> L. Tavora,<sup>16</sup> R. Terlizzi,<sup>5</sup> G. Vannini,<sup>30</sup> P. Vaz,<sup>16</sup> A. Ventura,<sup>36</sup> D. Villamarin,<sup>7</sup> M. C. Vincente,<sup>7</sup> V. Vlachoudis,<sup>4</sup> R. Vlastou,<sup>31</sup> F. Voss,<sup>19</sup> S. Walter,<sup>19</sup> M. Wiescher,<sup>18</sup> and K. Wisshak<sup>19</sup>

The n\_TOF Collaboration ([www.cern.ch/ntof](http://www.cern.ch/ntof))

<sup>1</sup>Istituto Nazionale di Fisica Nucleare, Sezione di Trieste, Italy – <sup>2</sup>CEA, Saclay, Irfu, Gif-sur-Yvette, France – <sup>3</sup>Istituto Nazionale di Fisica Nucleare, Sezione di Legnaro, Italy – <sup>4</sup>CERN, Switzerland – <sup>5</sup>Istituto Nazionale di Fisica Nucleare, Sezione di Bari, Italy – <sup>6</sup>Universidade de Santiago de Compostela, Spain – <sup>7</sup>Centro de Investigaciones Energeticas Medioambientales y Tecnológicas, Madrid, Spain – <sup>8</sup>University of Lodz, Lodz, Poland – <sup>9</sup>Centre National de la Recherche Scientifique/IN2P3 IPN, Orsay, France – <sup>10</sup>Atominstytut der Österreichischen Universitäten, Technische Universität Wien, Austria – <sup>11</sup>Centre National de la Recherche Scientifique/IN2P3 IREs, Strasbourg, France – <sup>12</sup>Faculty of Mathematics and Physics, Charles University in Prague, Czech Republic – <sup>13</sup>Universitat Politècnica de Catalunya, Barcelona, Spain – <sup>14</sup>International Atomic Energy Agency (IAEA), NAPC/Nuclear Data Section, Vienna, Austria – <sup>15</sup>Universidad de Sevilla, Spain – <sup>16</sup>Instituto Tecnológico e Nuclear (ITN), Lisbon, Portugal – <sup>17</sup>LIP Coimbra & Departamento de Física da Universidade de Coimbra, Portugal – <sup>18</sup>University of Notre Dame, Notre Dame, USA – <sup>19</sup>Karlsruhe Institute of Technology, Campus Nord, Institut für Kernphysik, Germany – <sup>20</sup>Instituto de Física Corpuscular, CSIC-Universidad de Valencia, Spain – <sup>21</sup>Aristotle University of Thessaloniki, Greece – <sup>22</sup>Joint Institute for Nuclear Research, Frank Laboratory of Neutron Physics, Dubna, Russia – <sup>23</sup>Institute of Physics and Power Engineering, Obninsk, Russia – <sup>24</sup>Centre National de la Recherche Scientifique/IN2P3 CENBG, Bordeaux, France – <sup>25</sup>Los Alamos National Laboratory, New Mexico, USA – <sup>26</sup>Tokyo Institute of Technology, Tokyo, Japan – <sup>27</sup>University of Ioannina, Greece – <sup>28</sup>Oak Ridge National Laboratory, Physics Division, Oak Ridge, USA – <sup>29</sup>NCSR, Athens, Greece – <sup>30</sup>Dipartimento di Fisica, Università di Bologna and Sezione INFN di Bologna, Italy – <sup>31</sup>National Technical University of Athens, Greece – <sup>32</sup>Institut für Fakultät für Physik, Universität Wien, Austria – <sup>33</sup>Pôle Universitaire Léonard de Vinci, Paris La Défense, France – <sup>34</sup>CEC-JRC-IRMM, Geel, Belgium – <sup>35</sup>Department of Physics and Astronomy, University of Basel, Switzerland – <sup>36</sup>ENEA, Bologna, Italy – <sup>37</sup>Università degli Studi di Pavia, Pavia, Italy

## Abstract

Neutron-induced fission cross-sections of  $^{233}\text{U}$ ,  $^{241}\text{Am}$  and  $^{243}\text{Am}$  relative to  $^{235}\text{U}$  have been measured in a wide energy range at the neutron time of flight facility n\_TOF in Geneva to address the present discrepancies in evaluated and experimental databases for reactions and isotopes relevant for transmutation and new generation fast reactors.

A dedicated fast ionization chamber was used. Each isotope was mounted in a different cell of the modular detector.

The measurements took advantage of the characteristics of the n\_TOF installation. Its intrinsically low background, coupled to its high instantaneous neutron flux, results in high accuracy data. Its wide energy neutron spectrum helps to reduce systematic uncertainties due to energy-domain matching problems while the 185 m flight path and a 6 ns pulse width assure an excellent energy resolution.

This paper presents results obtained between 500 keV and 20 MeV neutron energy.

## Introduction

Precise neutron-induced fission cross-sections of actinides are required for the design of systems based on the Th/U fuel cycle, for ADS, and Gen-IV nuclear reactors. Requests concerning the accuracy of  $\sigma(n,f)$  data are issued by the OECD/NEA nuclear science committee for some isotopes and reactor types [1].

An extensive measurement campaign for reducing the  $\sigma(n,f)$  uncertainties for major and minor actinide isotopes has been carried out at the n\_TOF neutron time of flight facility. In this contribution we report on the  $^{233}\text{U}$ ,  $^{241}\text{Am}$  and  $^{243}\text{Am}$  (n,f) cross-sections from 500 keV up to 20 MeV.

## Experimental set-up

### The n\_TOF facility

The n\_TOF (Neutron Time Of Flight) facility at CERN is based on a spallation neutron source, consisting of a  $80 \times 80 \times 60 \text{ cm}^3$  thick lead target, which is hit by a pulsed beam of 20 GeV/c protons with 6 ns r.m.s. and a typical repetition rate of 2.4 seconds.

A 185 m long evacuated beam pipe connects the target with the experimental area equipped with several detectors, assuring high energy resolution. The instantaneous neutron flux of  $10^5 \text{ n/cm}^2/\text{pulse}$  at the sample position makes the installation particularly suitable for high accuracy (n,f) cross-section measurements because of the favourable signal to noise ratio related to the natural alpha radioactivity of most actinides. A detailed description of the facility can be found for example in ref. [2] and references therein.

### The detector

Neutron-induced fission cross-section measurements have been performed using a Fast Ionization Chamber (FIC). The detector is a modular set of cells. Each cell is composed of three aluminium electrodes 12 cm in diameter which are separated by gaps of 5 mm filled with gas (90% Ar + 10%  $\text{CF}_4$ ) at a pressure of 720 mbar. The central electrode is 100  $\mu\text{m}$  in thickness and is plated on both sides with a fissile isotope matching the beam diameter, while the two outer electrodes are 15  $\mu\text{m}$  thick. An electric field of 600 V/m is obtained in the gaps by connecting the central electrode to the bias voltage and by keeping the outer ones at ground potential.

## Data analysis

Cross-sections are extracted relative to  $^{235}\text{U}$ , which is a standard between 0.15 MeV and 200 MeV. At high energy, the output signals of the FIC are strongly affected by the  $\gamma$ -flash, i.e. photons and other relativistic particles created in the spallation reaction. A software compensation technique [3] that subtracts the output of two adjacent electrodes was applied to extract the signals of fission



fragments. These were further subjected to a pulse shape analysis routine and an amplitude threshold selection to discriminate between fission fragments and  $\alpha$  particles.

The TOF information was converted to a neutron energy scale by defining the so-called “time zero” by means of the  $\gamma$ -flash. The “stopping time” was given by the fission fragment signals. The neutron-induced fission cross-sections are extracted according to Eq. (1):

$$\sigma_{x(n,f)} = \sigma_{235(n,f)} \cdot \frac{N_x}{N_{235}} \cdot \frac{m_{235}}{m_x} \cdot \frac{A_x}{A_{235}} \cdot c_f$$

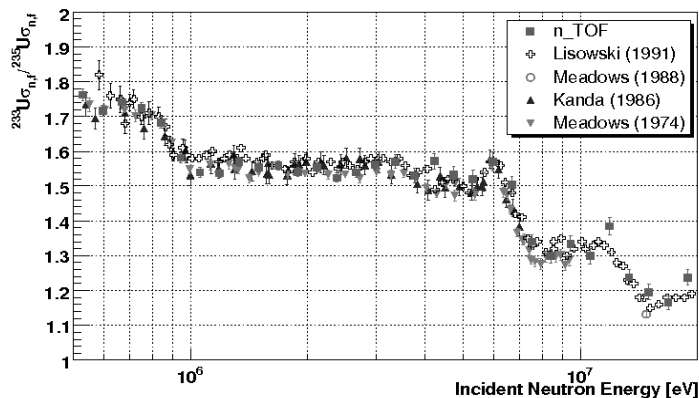
where  $\sigma_{235(n,f)}$  is the tabulated ENDF/B-VII.0 cross-section, x stands for the investigated isotope ( $^{233}\text{U}$ ,  $^{243}\text{Am}$  or  $^{241}\text{Am}$ ),  $N_x$  denotes the number of fission events detected for isotope x,  $m_x$  is the mass (in grams) of isotope x,  $A_x$  is the atomic number of isotope x and  $c_f$  is a correction factor accounting for dead time effects and detection efficiency. The dead time was treated as non-paralyzable, and the detection efficiency was estimated by simulating the energy loss of fragments in the gas with the FLUKA [4] code. Both corrections are of a few percent only and contribute less than 1% to the total uncertainty.

Considering all effects and corrections introduced in the measurement, the overall systematic uncertainty of the extracted cross-section is 3%. An important contribution is due to the uncertainty of the mass of the various deposits, which is 1.35% for  $^{235}\text{U}$  and 1.2% for all other isotopes. The statistical uncertainty is less than 2% for  $^{233}\text{U}$  in the whole energy range for a binning of 20 bins/decade and less than 3.5% in the case of  $^{243}\text{Am}$  (same binning) for neutron energies higher than 1 MeV. At lower energies, below the fission threshold, the poor counting statistics gives rise to a maximum uncertainty of 7.2%. A variable bin size was used to extract the neutron-induced fission cross-section of  $^{241}\text{Am}$ , where the statistical uncertainty is <2.9% for neutron energies above 1 MeV, and up to 9.5% below the fission threshold.

## Results

The n\_TOF results for  $^{233}\text{U}$  agree within 2.1% with the experimental data by Lisowski *et al.* [5], Meadows *et al.* [6] and Kanda *et al.* [7] (see Figure 1). The ENDF/B-VII.0 library is mainly based on these data, though for normalization purposes a “higher  $^{235}\text{U}$   $\sigma_{(n,f)}$  was used to produce better agreement with fast critical benchmark experiments” [8]. As a result, at  $E_n < 0.7$  MeV we confirm the experimental data reported in Figure 1 and the older ENDF-BVI.8 library, suggesting a revision of the ENDF/BVII.0 evaluation.

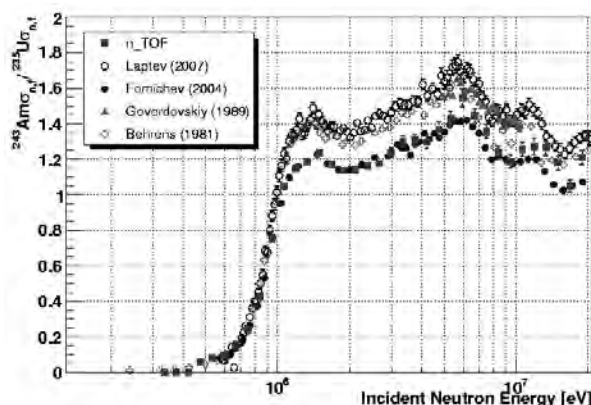
**Figure 1: Comparison among previous data and n\_TOF results for  $^{233}\text{U}$**



The fission cross-section data for  $^{243}\text{Am}$  tend to cluster in two distinct groups in the 1-6 MeV neutron energy range, separated by about 20% from each other (see Figure 2). The Laptev *et al.* [9] experimental data confirms the Goverdovskiy *et al.* [10] and the Behrens *et al.* [11], lying in the

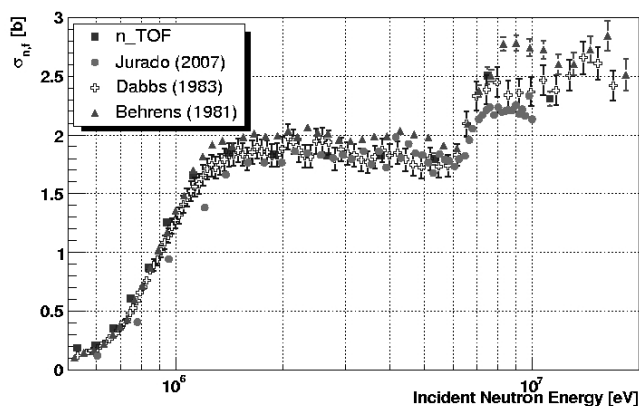
high energy cluster. The most recent experimental data set at the time of the ENDF/B-VII.0 release was by Laptev *et al.* [9] (information from [8]). Nevertheless such high cross-section values are in disagreement with the averaged cross-sections obtained in the ZEBRA reactor experiment [12], probably the reason why they have been discarded in the ENDF/B-VII.0 evaluation. The n\_TOF results confirm Fomichev *et al.* [13] and therefore the low energy cluster.

**Figure 2: Comparison among previous data and n\_TOF results for  $^{243}\text{Am}$**



In the case of the  $^{241}\text{Am}$  (n,f) cross-section the most recent experiment reported in EXFOR and ranging up to energies higher than 10 MeV is dated 1983 (Dabbs *et al.* [14]). The n\_TOF results agree rather well (within 3%) with this cross-section, confirming this data set rather than the older one by Behrens *et al.* [15]. Jurado *et al.* [16] experimental data suggest even lower cross-section values around 10 MeV (see Figure 3).

**Figure 3: Comparison among previous and n\_TOF results for  $^{241}\text{Am}$**



## Conclusions

Taking advantage of the high instantaneous neutron flux, the excellent resolution in neutron energy, and the low background of the n\_TOF facility, neutron induced fission cross-sections of  $^{233}\text{U}$ ,  $^{241}\text{Am}$  and  $^{243}\text{Am}$  have been measured with high accuracy over a wide neutron energy range.

## Acknowledgements

This work was supported by the EC under contract FIKW-CT-2000-00107 and by the funding agencies of the participating institutes.

## References

- [1] Nuclear Energy Agency (NEA), "Uncertainty and target accuracy assessment for innovative systems using recent covariance data evaluations", *International Evaluation Co-operation*, Vol. 26, NEA/WPEC-26, OECD/NEA, Paris (2008).
- [2] Belloni, F., et al., "Measurement of the neutron induced  $^{233}\text{U}$  fission cross-section in the energy range  $0.5 < E_n < 20$  MeV", in preparation (2010).
- [3] Colonna, N., et al., *Nucl. Instr. Meth. A*, in preparation, (2010).
- [4] Fassò, A., et al., *FLUKA: a multi-particle transport code*, Report numbers CERN-2005-10 (2005), INFN/TC\_05/11, SLAC-R-773.
- [5] Lisowski, P.W., et al., "Fission cross-section ratios for  $^{233,234,236}\text{U}$  relative to  $^{235}\text{U}$  from 0.5 to 400 MeV", *Proc. of the International Conference on Nuclear Data for Science and Technology*, Springer, p. 737, Juelich (1991).
- [6] Meadows, J., et al., "The Ratio of the Uranium-233 to Uranium-235 Fission Cross-Section", *Nucl. Science and Engineering*, 54, 317 (1974).
- [7] Kanda, J., et al., "Measurements of fast neutron induced fission cross-section of  $^{232}\text{Th}$ ,  $^{233}\text{U}$  and  $^{234}\text{U}$  relative to  $^{235}\text{U}$ ", *Radiation Effects*, 93, 233 (1986).
- [8] ENDF/B-VII.0, descriptive comments (2006).
- [9] Laptev, A.B., et al., "Neutron-Induced Fission Cross-Sections of  $^{240}\text{Pu}$ ,  $^{243}\text{Am}$  and  $^{\text{Nat}}\text{W}$  in the energy range 1-200 MeV", *Nucl. Phys. A*, 734, E45 (2004).
- [10] Goverdovskiy, A.A., et al., "Measurement of the Ratio of the Cross-Sections for Fission of  $^{243}\text{Am}$  and  $^{235}\text{U}$  by 5-10.5 MeV Neutrons", *Atomnaya Energiya*, 67, 30 (1989).
- [11] Behrens, J.W., J.C. Browne, "Measurement of the Neutron-Induced Fission Cross-Sections of Americium-241 and Americium-243 Relative to Uranium-235 from 0.2 to 300 MeV", *Nucl. Science and Engineering*, 77, 444, (1981).
- [12] Sweet, D.W., Report AEEW-R-1090 (1977).
- [13] Fomichev, A.V., et al., "Neutron Induced Fission Cross-Sections For  $^{240}\text{Pu}$ ,  $^{243}\text{Am}$ ,  $^{209}\text{Bi}$ ,  $^{\text{Nat}}\text{W}$  Measured relative to  $^{235}\text{U}$  in the Energy Range 1-350 MeV", *Khlopin Radiev Inst., Leningrad Reports No. 262*.
- [14] Dabbs, J., et al., "Measurements of the  $^{241}\text{Am}$  neutron fission cross-section", *Nucl. Science and Engineering*, 83, 22 (1983).
- [15] Behrens, J.W., et al., "Measurement of the Neutron-Induced fission cross-section of  $^{241}\text{Am}$  and  $^{243}\text{Am}$  Relative to  $^{235}\text{U}$  from 0.2 to 30 MeV", *Nucl. Science and Engineering*, 77, 444 (1981).
- [16] Jurado, B., et al., "Fission Cross-Sections and Fission-Fragments Mass Yields via the Surrogate Reaction Method", *Proceedings by Am. Inst. of Phys.*, No. 1005, p. 90 (2007).

